Water Secretion Associated with Exocytosis in Endocrine Cells Revealed by Micro Forcemetry and Evanescent Wave Microscopy

Takashi Tsuboi, Toshiteru Kikuta, Takashi Sakurai, and Susumu Terakawa*
Photon Medical Research Center, Hamamatsu University School of Medicine, Hamamatsu 431-3192, Japan

ABSTRACT It has been a long belief that release of substances from the cell to the extracellular milieu by exocytosis is completed by diffusion of the substances from secretory vesicles through the fusion pore. Involvement of any mechanical force that may be superposed on the diffusion to enhance the releasing process has not been elucidated to date. We tackled this problem in cultured bovine chromaffin cells using direct and sensitive methods: the laser-trap forcemetry and the evanescent-wave fluorescence microscopy. With a laser beam, we trapped a micro bead in the vicinity of a cell (with 1 μm of separation) and observed movements of the bead optically. Electrical stimulation of the cell induced many of rapid and transient movements of the bead in a direction away from the cell surface. Upon the same stimulation, secretory vesicles stained with a fluorescent probe, acridine orange, and excited under the evanescent field illumination, showed a flash-like response: a transient increase in fluorescence intensity associated with a diffuse cloud of brightness, followed by a complete disappearance. These mechanical and fluorescence transients indicate a directional flow of substances. Blockers of the Cl^- channel suppressed the rates of both responses in a characteristic way but not exocytotic fusion itself. Immunocytochemical studies revealed the presence of Cl^- and K^+ channels on the vesicle membranes. These results suggest that the externalization of hormones or transmitters upon exocytosis of vesicles is augmented by secretion of water from the vesicle membrane through the widened fusion pore, possibly modulating the rate and reach of the hormone or transmitter release and facilitating transport of the signal molecules in intercellular spaces.

INTRODUCTION

Release of neurotransmitters and hormones from cells involves exocytotic fusion of secretory vesicles with the plasma membrane. A pore is formed with a growing diameter as the membrane fusion proceeds. Consequently, the vesicle contents diffuse out through this fusion pore. The diffusion of small molecules in the water is believed to be fast enough to explain rapid chemical transmission in the synapse where the gap between the diffusional source and target sites is only 20 nm or less. Therefore, to date, no facilitatory mechanism has been proposed for the rapid transmission by exocytosis. In endocrine cells also, the release of hormones is believed to be completed by simple diffusion from the vesicular space to the extracellular space. In contrast, many exocrine cells are known to secret a large amount of water, which provides a vehicle for other secretes such as the mucus and the digestive enzymes to be transported through long ducts as in the salivary and the pancreatic glands. Thus, a reduced water release can result in a deterioration of the total secretory function that may lead to serious diseases, Shögrane syndrome, cystic fibrosis, and others to name a few. In the present study, we demonstrate that an endocrine (and neuroendocrine) cell also secrets water during its hormone- or transmitter-releasing activity.

Submitted March 7, 2001, and accepted for publication April 8, 2002.

Address reprint requests to Susumu Terakawa, Photon Medical Research Center, Hamamatsu University School of Medicine, 1-20-1 Handayama, Hamamatsu 431-3192, Japan; Tel.: 81-53-435-2092; Fax: 81-53-435-2092; E-mail: terakawa@hama-med.ac.jp.

0006-3495/02/07/172/12 $2.00

Many studies have suggested that secretory vesicles swell upon elevation of intracellular Ca^{2+} concentration (Finkelstein et al., 1986; Thirion et al., 1999). It was once thought that vesicle swelling triggered membrane fusion (Pazoles and Pollard, 1978; Pollard et al., 1980, 1984), the so-called "chemiosmotic lysis theory." However, membrane capacitance measurements and optical measurements in beige mouse mast cells revealed that swelling of vesicles occurs after membrane fusion and not before (Breckenridge and Almers, 1987; Zimmerberg et al., 1987). Even in much smaller secretory vesicles such as chromaffin vesicles, differential interference contrast (DIC) microscopy has shown that swelling of vesicles also occurs only after exocytotic fusion (Terakawa et al., 1991) and not before (Terakawa et al., 1993).

The chemiosmotic lysis theory failed to explain the molecular mechanism of initiation of exocytosis, and thus it has tended to be forgotten recently. Nevertheless, the involvement of the chemiosmotic response per se has not been excluded completely from the process of exocytosis. For example, the light scattering measurements of a suspension of secretory vesicles showed that the average vesicle diameter increased in a Ca^{2+}-dependent manner (Warashina, 1985; Miyamoto and Fujime, 1988), and electron microscopic studies showed that vesicles in the cytoplasm swelled by 10% on average when the cells were stimulated (Grant et al., 1987), and that they swelled significantly during the course of exocytosis (Ornberg et al., 1995).

The mechnochemical aspect of exocytosis has remained difficult to study in living endocrine and neuroendocrine cells. We used two optical techniques developed recently to shed light on the process taking place after the fusion event:

the laser trapping of a small bead (Gelles et al., 1988) and the evanescent wave illumination with total internal reflection (Stout and Axelrod, 1989; Steyer et al., 1997; Tokunaga et al., 1997; Oheim et al., 1998; Schmoranzer et al., 2000; Toomre et al., 2000). The former provided strong evidence for a micro force exerted by the cell upon exocytosis. The latter technique, which was further improved by using a high numerical aperture (NA = 1.65) objective lens (Terakawa et al., 1997), revealed a flow of a fluorescent probe from the vesicle. Here, we demonstrate that the release of hormone or transmitter from the endocrine cell occurs by diffusion heavily modified by a convective flow of water.

MATERIALS AND METHODS

Cell preparation and stimulation

Chromaffin cells were isolated from the bovine adrenal medulla by the collagenase digestion method (Waymire et al., 1983). The tissue was incubated for 90 min in Ca^{2+}- and Mg^{2+}-free culture medium containing collagenase (type I, Sigma, St. Louis, MO) at 4 mg/mL. The culture medium was Dulbecco's modified Eagle's medium (Life Technologies, Inc., Rockville, MD) supplemented with 10% fetal bovine serum (Life Technologies). Dissociated cells were cultured in a glass-bottomed petri dish (35 mm in diameter) under 5% CO_2 and 95% air at 37°C for 2 to 5 days. The dish was mounted on a microscope stage and warmed to 34.0 ± 2.0°C with an electric heater (nichrome wire insulated with a silicone tube) attached to the oil-immersion objective lens. The recording medium contained; 135 mM NaCl, 5.0 mM KCl, 2.0 mM $CaCl_2$, 1.0 mM $MgCl_2$, 10 mM Na-HEPES, 10 mM glucose (pH adjusted to 7.3). When necessary, botulinum neurotoxin C (BoTX/C, Wako Pure Chemical, Osaka, Japan) was added to the culture medium at a concentration of 1 μM. For evanescent wave microscopy, the cells were stained with 3 μM acridine orange (Sigma) added to the recording medium for 5 min at 34.0 ± 2.0°C, then rinsed with dye-free recording medium for 20 to 60 min. Superoxide dismutase (5 μM) and catalase (1 μM) were added to the recording medium to reduce adverse photodynamic effects during fluorescence observation. In most cases, the chromaffin cells were stimulated with current pulses applied through a micropipette attached to the cell surface. The micropipette (0.5–1 μm in diameter) was filled with the recording medium. The stimulating pulse, 1 to 2 μA in amplitude and 1 ms in duration, was supplied to the pipette through Ag/AgCl wire from the isolated output of a pulse generator (SEN-2201, Nihon Kohden, Tokyo, Japan). Such a stimulus induces an action potential (Brandt et al., 1976) and a long lasting (10–30 s) Ca^{2+} transient in the chromaffin cell. In a few cases, 60 mM NaCl in the recording medium was replaced with KCl for 2 min to stimulate the cells.

Laser trapping

According to the original method (Gelles et al., 1988), a polystyrene bead (1.0 or 2.0 μm in diameter; Sigma) was captured with a focused laser beam of 1064 nm in wavelength (from a Nd-YAG laser; 350 mW, Laser Compact Co, Ltd., Moscow, Russia). A laser beam from the Nd-YAG laser was expanded with a concave lens ($f = -50$ mm; Spindler and Hoyer, Göttingen, Germany). The expanded beam was then converged with a convex lens ($f = 150$ mm; Spindler and Hoyer) to fill the back aperture of the objective lens. By adjusting the position of convex lens axially, the focal point of 1064-nm beam could be varied in reference to the focal point of the visible light.

Before the laser-trapping experiment, a profile of the cell was determined by focusing on the foot region and then on the peak region of the cell in a DIC mode. After reading the micrometer scale of focusing knob, the bead was held at the peak level and then moved down to a level 1 μm above the surface of the foot region. During the experiment, the bead was held at this level (see, Fig. 1 *A*, inset). The effective laser power at the trapping point was kept at 53 mW for the whole measurements. When the bead touched the cell, it was difficult to detach and to shift it sideways with this laser power because of a strong adhesion. This helped us confirm the absence of direct contact of the bead with the cell.

The DIC image of the bead was observed with a visible (white) light and recorded continuously through an infrared cutoff filter with a CCD camera (C2400-75, Hamamatsu Photonics, Hamamatsu, Japan) at a 33-ms interval. The DIC image of the bead in the focus consisted of a complimentary pair of bright and dark crescents surrounded by a darker circle. When the bead moved in the *z* direction, one of the crescents increased its area and the other decreased, depending on the direction of the movement. This resulted in a change in brightness of the bead image. We measured the movements of the bead along the *z* axis by recording the changes in the light intensities of the center of the bead. Calibration for the bead movement was obtained by fixing a bead (2 μm in diameter) on the bottom of the dish and shifting, instead, the objective lens by a known distance to measure the brightness in the center of the bead. For a high-resolution measurement, an avalanche photodiode was used in the place of video camera.

In a few cases, a polystyrene bead was held above the cell not by laser trapping but by attaching it to the tip of a very fine glass pipette (<0.1 μm). The position of the bead was adjusted with a micromanipulator (MX630R, Newport, Irvine, CA) holding the glass pipette.

We determined the displacement response of the trapped bead by running a data analysis software package (Origin, OriginLab Corporation, Northampton, MA) in a personal computer. A peak-detection filter in the software was used with discriminators setting at a rate of rise of 100 nm per 2-point and at a threshold level of 100 nm. These parameters were kept unchanged for a series of data analysis.

Evanescence microscopy

A high numerical aperture objective lens (HR, Apochromatic, 100×, NA = 1.65, infinity corrected; Olympus Optical Co., Tokyo, Japan; originally developed by S. Terakawa and K. Abe) was mounted on a nosepiece of an inverted microscope (IX70, Olympus). A liquid (Cargille Laboratories, Cedar Grove, NJ) of a high refractive index ($n = 1.78$) was used to couple the lens to a coverslip. The coverslip was made of glass of the same refractive index ($n = 1.78$). A laser beam from a diode pumped solid-state laser (wave length = 532 nm, 50 mW; Excellence, Taipei, Taiwan) was expanded with a concave lens ($f = -15$ mm; Spindler and Hoyer). The expanded beam was focused with a convex lens ($f = 150$ mm; Spindler and Hoyer) on the back focal plane of the objective lens. A surface mirror was inserted in this optical path to aim the beam at the rim of the lens. The beam was incident on the front focal point of the lens with a large angle of incidence so that the beam was totally reflection there at the water-glass interface, creating the evanescent field in the water phase (Tokunaga et al., 1997).

The critical angle in our 1.65-NA lens was 50.83° and the widest possible (rim) angle was 67.97°. We usually aimed the laser beam at the middle range between these angles. At an angle of incidence $\theta = 60.0$ (deg), the decay length (d) of the evanescent field calculated by the following formula was 54.3 nm.

$$d = \frac{\lambda}{4\pi\sqrt{n_2^2 \sin^2\theta - n_1^2}}$$

in which n_1 is the refractive index of water (1.33), n_2 the refractive index of the coverslip (1.78), and λ the wavelength of laser (532 nm). A layer of 100 ~ 200 nm is the reach of the evanescent light.

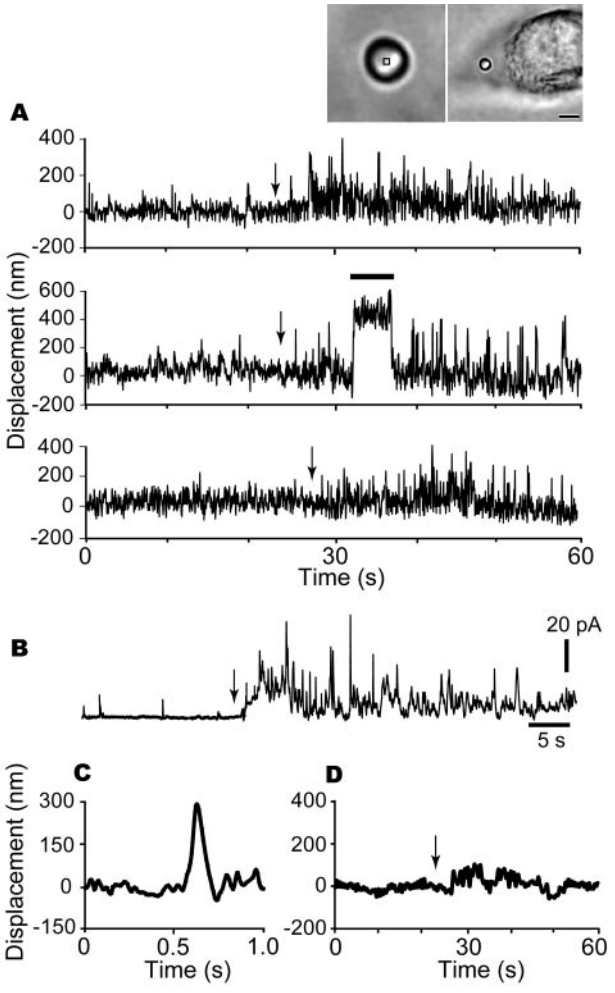

FIGURE 1 Micro forces exerted by a single chromaffin cell measured with a bead trapped in the medium with laser tweezers. (*A*) Displacement of the bead measured with the video system. (*Top*) Typical motion of the bead observed in the normal recording medium. The ordinate indicates the displacement of the bead in the *z* direction (upward deflection). (*Middle*) Bead was shifted by ~2 μm further from the cell (horizontal bar) during the exocytotic responses. A deflection of ~400 nm during this manipulation was due to the color aberration (between 1064 nm light for laser trapping and the visible light for DIC observation) of the objective lens. (*Bottom*) Displacements of the bead observed with the bead attached to a micro glass pipette. Arrows indicate electrical stimulation (1 ms, single pulse). (*Inset*) DIC image of the microbead laser-trapped above the cell (*right*) and its magnified image (*left*). Note dark and bright crescents obliquely aligned on the bead (*left*). A square in the center of bead indicates the region for intensity measurement. The calibration bar in the right represents 2 μm. (*B*) Current spikes recorded with a carbon fiber electrode attached to the cell; each represents a single quantum of catecholamine release. Secretion started when the electrical stimulation was applied (*arrow*). (*C*) Displacement of the bead observed in an expanded time scale. An avalanche photodiode was used to record the brightness of the bead in the DIC mode, which was then converted to the displacement. (*D*) Slow component of the bead-displacement response obtained by low-pass Fourier filtering (frequencies higher than 1 Hz were suppressed). The arrow indicates time of electrical stimulation.

A dichroic mirror was also inserted in the optical path to filter out a fluorescence signal from the cell. The fluorescence of the cell observed with the 1.65-NA lens was more than fivefold brighter compared with that observed with a 1.40-NA lens. The fluorescence image was recorded at the video rate with an ICCD camera (DAS-512, Imagista, Tokyo, Japan) combined with an image intensifier (VS4-1845, VideoScope, Sterling, VA). Video images were contrast-enhanced with a digital image processor (ARGUS-20, Hamamatsu Photonics), and recorded on digital videotape (WV-D10000, Sony, Tokyo, Japan). Images were reproduced from the videotape by digitizing the proper frames using a personal computer (Power Macintosh G4/450, Apple Computer, Inc., Tokyo, Japan) and by printing them with a digital graphic printer (UP-D8800, Sony).

The fluorescence intensity of a single vesicle was measured with a back-illuminated CCD camera (88 × 80 resolution, 16-bit accuracy; Neurocam, Life Science Resources, London, UK) operated at a frame rate of 4.5 ms. The magnification of the optical image was adjusted in such a way that one pixel of this CCD camera covered almost the whole area of a single vesicle. Sequential images obtained with the back-illuminated CCD camera were stored on a personal computer (Dell, Tokyo, Japan). Sequential image data were analyzed with an image-processing program (Merlin, Life Science Resources, London, UK).

DC amperometry

A carbon fiber electrode (8 μm) insulated with a glass capillary was used to monitor the release of the catecholamine from individual chromaffin vesicles. The electrode was gently attached to the surface of the cell. An Ag/AgCl electrode immersed in the chamber served as a reference electrode. An oxidization current was measured by holding the potential of the carbon electrode at +500 mV in reference to the bath potential using an amperometric amplifier (Micro C, World Precision Instruments, Sarasota, FL). The oxidization current was digitized with an A/D converter (PowerLab/8sp, Adinstruments Japan, Inc., Tokyo, Japan), and recorded in a PC/AT computer using software (Chart, Adinstruments).

Immunoblotting

Rat and bovine adrenal chromaffin cells were homogenized in solution containing 150 mM NaCl, 50 mM Tris-HCl (pH 7.5), and a set of protease inhibitors (5 mM EDTA, 1 mM phenylmethylsulfonyl fluoride, 2 mM *N*-ethylmaleimide, 1 μg/mL leupeptin, and 1 μg/mL pepstatin A) at 4°C. The cell homogenate was sonicated for 5 s and centrifuged at 24,000 × *g* for 30 min at 4°C. The precipitate was resuspended in the same solution to make 10 μg/μL protein. This protein solution (2 μL) was added to 1 mL of sodium dodecyl sulfate-sample buffer (62.5 mM Tris-HCl, 2 mM EDTA, 2% (w/v) sodium dodecyl sulfate, 10% (w/v) glycerol, 0.001% (w/v) bromophenol blue, and 80 mM dithiothreitol). The sample was electrophoresed on 8% sodium dodecyl sulfate-polyacrylamide gel and transferred to a nitrocellulose membrane. The nitrocellulose membrane was treated with 5% skimmed milk solution for 3 h at room temperature and then incubated with rabbit anti-rat ClC-3 polyclonal antibody (Alomone Labs, Jerusalem, Israel) for 12 h at 4°C. After this procedure, the membrane was incubated in medium containing 100-fold diluted peroxidase-conjugated goat anti-rabbit immunoglobulin G (Dako Japan Co. Ltd., Tokyo, Japan) antibody for 1 h at room temperature. After a final rinsing, immunoreactive bands were developed by using POD immunostaining set (Wako Pure Chemical inc. Ltd., Osaka, Japan).

Immunofluorescent staining

Cells cultured on the coverslip were fixed in 99.5% ethanol for 10 min at 4°C and then rinsed in 0.01% Triton X100-containing phosphate-buffered saline (TBS). After fixation, the cells were treated with 1% skim milk-containing TBS, and incubated with rabbit anti-rat ClC-3 polyclonal antibody (Alomone Labs) or rabbit anti-rat Ca^{2+}-dependent K^+ channel poly-

clonal antibody (Alomone Labs) for ~1 h at room temperature. After washing in TBS, the cells were incubated with fluorescein isothiocyanate-conjugated goat anti-rabbit immunoglobulin G (Southern Biotechnology Associates, Inc, Birmingham, AL) for 12 h at 4°C. After a final washing, the cells were observed with a confocal microscope equipped with a microlens-attached Nipkow-disk scanner (CSU-10, Yokogawa Electric Co., Tokyo, Japan).

RESULTS

Volume flow of water associated with the exocytotic response

We measured the volume flow of water directly during the exocytotic response by the optical trapping technique. A micro bead was held ~1 μm above the flat surface of a chromaffin cell (Fig. 1 *A*, inset). The bead was trapped in a stable manner despite the disturbance by Brownian movement of water molecules. Application of a stimulating electrical pulse to the cell induced many small movements of the bead along the *z* axis observed as changes in light intensity of the bead in the DIC mode.

The movements consisted of rapid transient displacements from the trapping center superposed on slower displacements (Fig. 1 *A*, top). The rapid transients measured in an expanded time scale (Fig. 1 *C*) indicated a rise time of ~50 ms and a duration of 200 to 500 ms. The fastest velocity calculated was 6 μm/s. A signal processing with the Fourier filtering method revealed a slow component lasting a few tens of seconds (Fig. 1 *D*). Both the rapid and the slow displacements appeared in the upward direction, indicating a positive force directed from the cell surface to the external medium. These responses continued for 20 s or more after the electrical stimulation. The light intensities measured in the video pixels aiming at the spaces slightly off from the bead showed no significant changes. When the trapping center for the bead was shifted by ~2 μm further from the cell by moving the objective lens, electrical stimulation induced no significant movement of the bead (Fig. 1 *A*, middle). Therefore, the movement of the bead reflected transient forces exerted by the cell within the space ~1 to 2 μm distant from its surface. The displacements measured with a 1-μm bead tended to be larger and noisier than those measured with a 2-μm bead, reflecting a difference in trapping force. When the laser power was reduced to the level near the escaping point of trap, large displacements of the bead were observed also. However, the baseline was very noisy and the bead, in fact, escaped easily from the trap (data not shown). To exclude the possibility that the changes in light intensity arose from fluctuations of the bead-trapping laser beam, the same measurements were performed with the bead held above the cell with a fine glass pipette. Similar transient and irregular displacements of the bead appeared after electrical stimulation (Fig. 1 *A*, bottom).

Recording of quanta of catecholamine release by the carbon fiber DC-amperometry revealed that significant secretion occurred for a long time after the electrical stimulation with a short current pulse (Fig. 1 *B*). The time course of whole secretory responses was in agreement with that of force responses measured with the bead. The time course of a single quantum was also very similar to the rapid transient of bead displacement measured in an expanded time scale (Fig. 1 *C*).

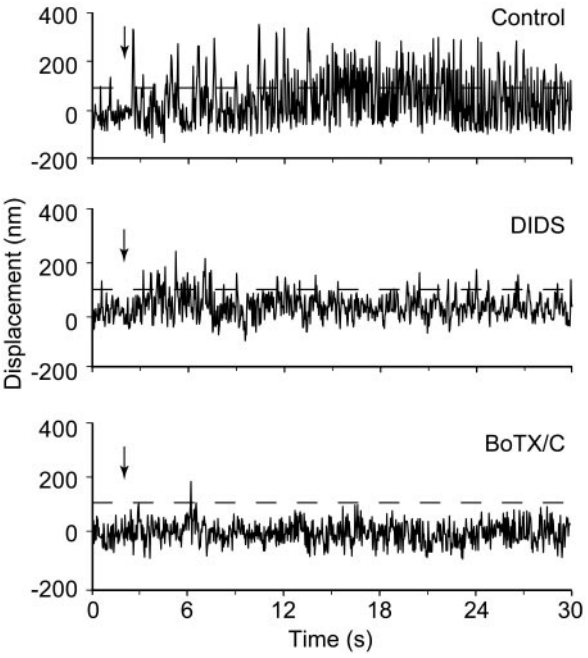

FIGURE 2 Effects of DIDS and botulinum neurotoxin on the generation of the micro force. Displacements observed in control (*top*), in medium containing 100 μM DIDS (*middle*), and in medium containing 1 μM botulinum neurotoxin C (*bottom*). Arrows indicate the time of electrical stimulation. Broken lines indicate a threshold level for signal discrimination. Peaks were further discriminated by their rate of rise (see Materials and Methods).

Effect of chemicals on the volume flow

The application of 4,4′-diisothiocyanostilbene-2,2′-disulphonate (DIDS, 100 μM), a blocker of the voltage-dependent Cl^- channel (Best et al., 2000), to the cell for 10 min reduced the amplitudes and the numbers of the displacements (Fig. 2). Not only spiky responses but also slow components were suppressed by DIDS. The suppression was not complete, yet prolonged application did not further increase the effect. Histograms of the bead displacements were obtained to establish the effect of DIDS (Fig. 3). Mainly, large displacements were eliminated. The average bead displacement decreased from a control value of 201 ± 45 nm (mean ± SD, $n = 134$ events) to 144 ± 35 nm ($n = 47$ events) after DIDS application. The difference was statistically significant at $p < 0.05$ (*t*-test). Application of botulinum neurotoxin C (a protease of synaptosome-associated protein of 25 kDa: SNAP-25 and syntaxin) to the cell

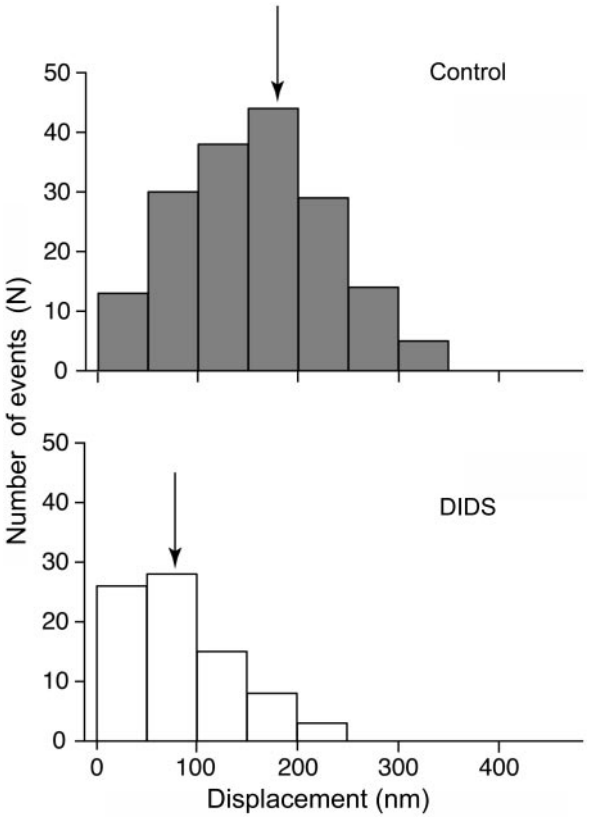

FIGURE 3 Frequency histograms of the transient displacements of the bead. Displacements observed in control medium (*top*) and in medium containing 100 μM DIDS (*bottom*). Arrows indicate the mean values of the displacements. A bead of 2 μm in diameter was used.

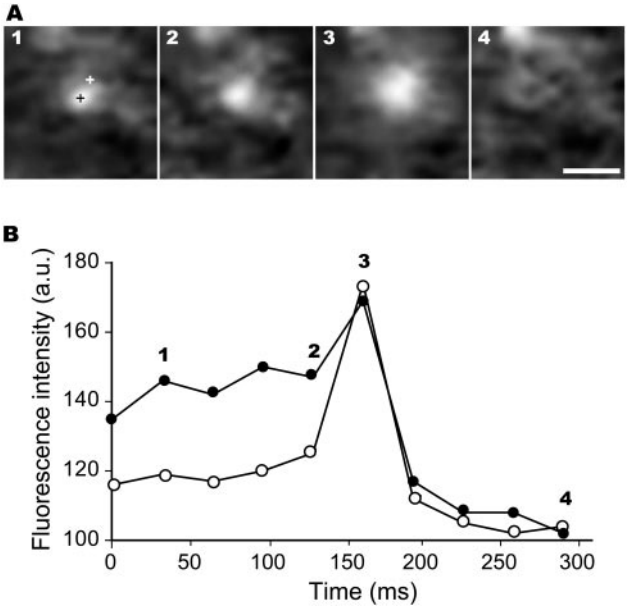

FIGURE 4 Images of exocytosis of a vesicle observed under evanescent field illumination at 15 s after electrical stimulation. (*A*) images of a single vesicle reproduced from video frames at 33-ms intervals (1–4). Image 3 shows a diffuse cloud of the dye and image 4 shows the abrupt disappearance of the fluorescent spot. Bar = 1 μm. (*B*) Time courses of the fluorescence changes measured in the center (*black crosses* and *filled circles*) and at the edge (*white crosses* and *open circles*) of the vesicle shown in *A*. The numbers in the frames correspond to those in *A*. The fluorescence intensities are expressed in the 8-bit value of digitization.

for 6 h suppressed the generation of the pulse-like force transient completely (Fig. 2, bottom). Therefore, the force transients were closely associated with the exocytosis.

Evanescence fluorescence images

To substantiate the volume flow further by a completely different method, we observed the exocytotic release of a fluorescent probe from vesicles under an evanescent field illumination. Secretory vesicles loaded with acridine orange were clearly visualized as brightly fluorescent spots (Fig. 4 *A*). The cells had 1.1 $\pm$ 0.2 (n = 82 cells) fluorescent spots per square micron, similarly to a previous observation (Steyer et al., 1997). After application of a single pulse to a cell, 76 $\pm$ 8% of the vesicles initially seen disappeared one after another during ~30 s (46 cells). These changes were attributed to exocytosis.

In most exocytotic responses, a diffuse cloud of dye replaced the vesicles for a brief time (33–100 ms) immediately before their disappearance. The transient appearance of the cloud gave a flash-like impression (we will refer to it as flash-type response; Fig. 4 *A*, images 2, 3). The momentary cloud was mostly circular (occasionally irregular), its diameter was approximately twice that of the vesicle, and it was associated with a marked increase in brightness (Fig. 4 *A*, image 3). However some fluorescent vesicles disappeared without showing any cloud or flash (simple type). The fluorescence intensities (FI) were measured from the sequence of video images by digitizing the pixel values in the center and at the edge of a single vesicle (Fig. 4 *A*). When the diffuse cloud appeared, time plots (Fig. 4 *B*) showed that the FI at both points increased transiently, which was consistent with the impression of the flash. After this release response, the FI of both points decreased. In the center of the vesicle, the differences in FI between the initial and the final levels were large (filled circles in Fig. 4 *B*). The transient increases in FI (spike) in the center were also quite variable. In contrast, in the area outside the fluorescent spot (open circle in Fig. 4 *B*) the differences in FI between the initial and the final levels were smaller, although the transient increase was larger.

The most probable interpretation of these findings is that the fluorescent molecules were ejected from the secretory vesicles by some force additional to the diffusion. Such a force rapidly drives the probe molecules closer to the glass surface before they diffuse away. While these molecules are traveling in the region where the evanescent field is strong, the fluorescence intensity increases transiently (see Discussion and Appendix).

Time-resolved evanescence fluorescence images

To measure the fast dynamics of the release process in individual secretory vesicles, the FI of vesicles were recorded with a high-speed back-illuminated CCD camera (Fig. 5 *A*, left). After electrical stimulation, the FI signals in many vesicles showed a brief increase (spike) followed by a persistent decrease. In search of a hidden component other than the obvious spike, we averaged these FI signals obtained from 50 vesicles and made a time differentiation of the spike time course at 4.5-ms resolution. Only one peak was found in the rising phase of the spike (Fig. 5 *A*, right), indicating that the transient increase in FI has a single component.

The increments in FI among the vesicles were variable (Fig. 5 *A*, left). We measured the amplitudes of the initial spikes (S) and the following decrements (D) (see Fig. 5 *A*, left, for definition), and statistically examined the ratio of the initial spike to the stepwise decrease (S/D ratio) in many vesicles. The ratio varied in the range of 0 to 5 (Fig. 5 *B*). Approximately 15% of vesicles showed little or no transient increase in fluorescence. We defined a response with a S/D ratio greater than 1 as the flash type and a response with a ratio less than 1 as the simple type.

To compare the results to those obtained by conventional methods, we examined the acridine orange-stained chromaffin cells using a conventional epifluorescence microscope and a confocal microscope. Electrical stimulation induced disappearance of many fluorescent vesicles with time-courses similar to those described above. However, under the epifluorescence microscope, no transient increase was observed before the decreases in vesicle fluorescence (Fig. 5 *C*). Under the confocal microscope, only a few (less than 10%) vesicles showed a small spike (Fig. 5 *C*) with the S/D ratios all less than 0.8 (Fig. 5 *B*). The S/D ratio is an indicator for the strength of the ejecting force exerted on the probe molecules. It depends on the profile of excitation field also. Because of an extremely steep slope, the evanescent field illumination is the most advantageous method for estimating the ejection force working in the exocytotic release.

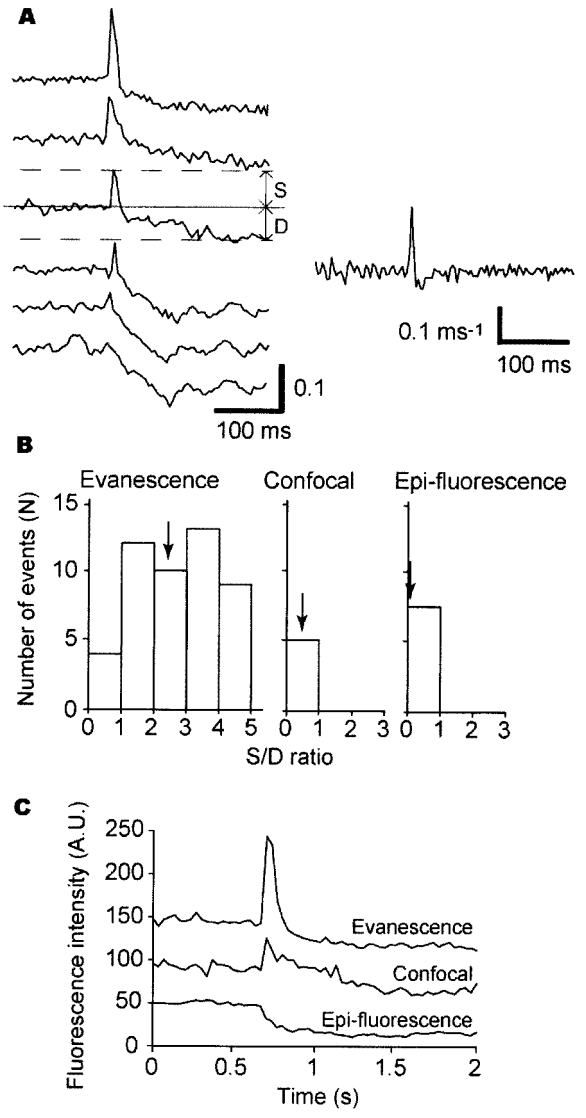

FIGURE 5 Changes in fluorescence intensities of a single vesicle during exocytosis. (*A*) Fluorescence intensity change of the vesicles measured with high speed CCD camera. (*Left*) Fluorescence intensity signals of six vesicles recorded with the high speed CCD camera (4.5 ms of time resolution). S and D indicate the initial spike and the stepwise decrease in fluorescence signal. (*Right*) Time derivative of an averaged fluorescence intensity signal obtained from many vesicles ($n = 50$) that showed the spike response as shown in the left panel. The time derivative curve was made by subtracting a fluorescence intensity of a time point from that of a previous time point (4.5-ms interval). The highest peak in each signal was used as a reference point for averaging along the time scale. The averaging would increase the peak-detection sensitivity sevenfold. (*B*) Histograms of the ratios of the initial spike (S) to the stepwise decrease (D) obtained by evanescence microscopy, confocal microscopy, and conventional epifluorescence microscopy. Arrows indicate the mean S/D values. (*C*) Fluorescence intensity signals of an exocytotic response of a single vesicle obtained by different microscopic methods (33-ms resolution). One of the largest spikes is shown for each method. Traces are arbitrarily shifted along the ordinate to avoid overlapping.

Effect of chemicals on the fluorescence image

The effects of several pharmacological agents were examined by measuring their actions on the incidence of flash type responses observed in a unit time of 10 s by evanescent-field microscopy (Fig. 6). An average of 87% of the exocytotic responses was the flash type (46 cells). Application of charybdotoxin (ChTX, 25 nM, a blocker of the Ca^{2+}-dependent K^+ channel) decreased the proportion of flash type exocytotic responses slightly without changing the sum of flash type and simple type. In other experiments, bafilomycin A (100 nM, a blocker of vesicular H^+-ATPase), was applied to the cell for 10 min before the cells were stimulated. It reduced the number of exocytotic events (in a unit time of 10 s) but did not affect the proportion of

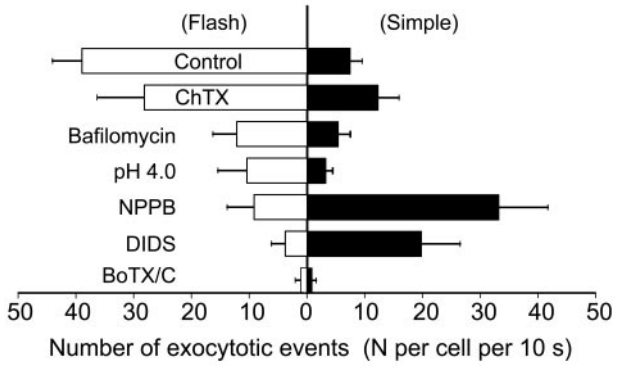

FIGURE 6 Effects of chemicals on the flash response and the S/D ratio. Flash-type response was inhibited by chloride channel blockers. The number of exocytotic responses in a single cell in 10 s (mean ± SD) after electrical stimulation is shown with a distinction between the flash type (*open bar*) and the simple type (*filled bar*).

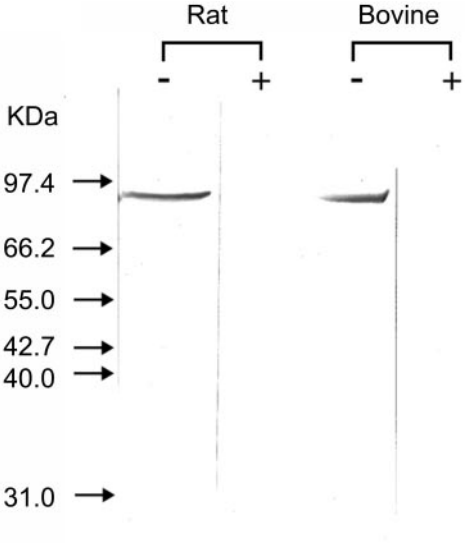

FIGURE 7 Expression of Cl^- channel (ClC-3) in rat and bovine chromaffin cells. Anti-ClC-3 recognized a single band (85 kDa) both in rat and bovine chromaffin cells. +, Preabsorbed anti-ClC-3 antibody was present. −, Preabsorbed antibody was absent. The positions of molecular weight makers are indicated.

the flash type to the simple type. The extracellular medium buffered to pH 4.0 showed the same results. The addition of 5-nitro-2-(3-phenylpropylamino)-benzoic acid (100 μM), a blocker of the cystic fibrosis transmembrane conductance regulator (Walsh et al., 1999), decreased the proportion to 25% without changing the sum of flash type and simple type. In the presence of DIDS (100 μM), the proportion decreased to 20% with only a slight decrease in number of responses (in a unit time of 10 s). In several cells examined, the proportions of the flash type responses were increased slightly when the medium was replaced with a hypotonic solution (NaCl concentration reduced by 50%) or with a gluconate solution (two-thirds of the chloride replaced with gluconate) (data not shown). Botulinum neurotoxin C (1 μM) inhibited both the flash type and the simple type responses completely after 6 h, indicating that the both responses were exocytosis.

Localization of the Cl^- and K^+ channels

To gain an insight further into the large effect of chloride channel blockers (on the transient force response and the fluorescence response) mentioned above, we investigated the presence and distribution of the chloride channels in the chromaffin cells. An antibody against the voltage-gated Cl^- channel, ClC-3 (Kawasaki et al., 1994), was used for an immunoblot and immunocytochemical staining. On the immunoblot of rat and bovine chromaffin cells, the antibody identified only a single band at 85 kDa. Anti-ClC-3 antibody preabsorbed with antigenic peptide (1 μg/mL) blocked staining of ClC-3 protein (Fig. 7). The ClC-3 staining in the cell preparation showed a particulate or punctured pattern representing many secretory vesicles with a variable density (Fig. 8 *B*). These findings indicate that the Cl^- channels are densely distributed on the vesicle membrane.

Ca^{2+}-dependent K^+ channels have been reported to be present on the vesicle membrane (Stanley and Ehrenstein, 1985; Ashley et al., 1994). We confirmed this in our cells using an antibody against the K^+ channel. The immunostaining showed particulate images very similar to that of

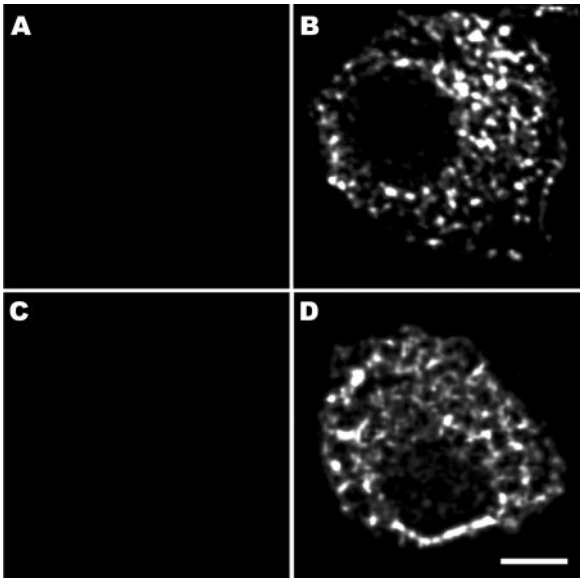

FIGURE 8 Confocal micrographs of immunocytochemical localization of voltage-gated Cl^- channel (ClC-3) and Ca^{2+} -dependent K^+ channel in the bovine adrenal chromaffin cell. (*A*) Anti-ClC-3 antibody was absent. (*B*) Anti-ClC-3 antibody was present. (*C*) Anti-Ca^{2+}-dependent K^+ channel antibody was absent. (D) Anti-Ca^{2+}-dependent K^+ channel antibody was present. Scale bar = 5 μm.

the Cl^- channel distribution (Fig. 8 *D*), indicating that the K^+ channels were also present on the vesicle membrane.

DISCUSSION

Movements of the bead

We believe that the movements of the bead observed near the chromaffin cell during exocytotic responses are not artifacts for the following reasons. The shapes, polarities, and durations of the movement were similar among preparations and did not vary with changes in stimulus strength (current density of the stimulating pulse). When the position of the bead was shifted by ~2 μm further from the cell, there was no movement during the exocytotic response. The movements of the bead were suppressed by application of DIDS and botulinum neurotoxin C to the cell. The suppressive effect of this toxin on the exocytosis in the same cells was established earlier by patch-clamp measurements of the membrane capacitance (Xu et al., 1998). These findings support the view that the exocytotic release of substances from a vesicle is driven by a transient volume flow of water. The slow components probably reflect a continued secretion of water through the open mouth of fused granules.

Flash response

Under the conventional epifluorescence microscope, there was no flash response when the fluorescently labeled vesicles disappeared (i.e., S/D = 0). If the flash response arose from a chemical or an environmental change that influenced the quantal efficiency of fluorescence of the probe, the S/D ratio in different microscopy modes should not vary. The large S/D values found only by evanescence microscopy were due to the extraordinary steep gradient of the illumination field. Because such a field served as a very sensitive scale for the movement of fluorescent objects, the flash response or the transient increase in fluorescence very likely represented the translocation of the fluorescent probe from a place (secretory vesicle) 100-nm distant from the glass substrate to a place very close to it (outside the cell). Flash responses very similar to those described here were observed also in MIN6 cells of which granules contained no acridine orange but insulin fused with the green fluorescent protein (Ohara-Imaizumi et al., 2002).

A time derivative of the fluorescence intensity signal showed a monotonically rising peak, indicating that only one component was involved in the signal (Fig. 5 *A*, right). If this component is due to a movement of vesicle against the exponential slope of the evanescent field, the calculated velocity of the vesicle movement would reach an unrealistic value (~15 μm/s). This value is much higher than those described previously for the same cell (Steyer et al., 1997). Accordingly, we regarded the spike in fluorescence signal simply as a release of acridine orange from the vesicle toward the glass (and not as translocation of the vesicle itself) and not as two steps including a vesicle movement followed by an exocytotic release.

Release of the fluorescent molecules from the vesicle by simple diffusion would result in dilution of molecules in the extracellular space immediately after their externalization. Thus, the fluorescence images of vesicles simply disappear upon exocytosis despite the advancement of molecules into a stronger field of excitation. In contrast, when the ejecting force is large and dominating over the diffusion, the fluorescent molecules distribute more in the region (near the surface of coverslip) where the evanescent field is stronger. This rapid transport of fluorescent molecules from the vesicle to the field of a high intensity creates the flash or a transient increase in fluorescence intensity. A simulation of the molecular release underlying the flash response is included in Appendix.

pH dependence

Acridine orange is known to be a pH sensitive dye. Because the lumen of a vesicle is highly acidic, exocytosis would be associated with an abrupt rise in pH. In fact, a pH-sensitive green fluorescent protein targeted to the cytosol, mitochondria, and trans-Golgi showed a change in fluorescence upon stimulation (Llopis et al., 1998). Such a pH change could be an alternative cause for the flash response. However, our results excluded this possibility. First, the pH dependence of the fluorescence intensity of acridine orange (see Appendix) was too small to account for the large spike, which usually had a more than 100% increase. Second, bafilomycin A, which is known to inhibit vacuolar H^+-ATPase (Bowman et al., 1988) and thus would raise the intravesicular pH, did not affect the ratio of the number of flash responses to the number of simple responses (flash/simple ratio) in a cell (Fig. 6). Third, the value of the S/D ratio showed little or no change in cells immersed in a low-pH medium in which the dye would not be subjected to a significant change in pH upon exocytosis (Fig. 6). Therefore, the flash response must reflect the spatial displacement of the probe and not the pH dependence of the quantal efficiency.

Self quenching

Some fluorescent dyes are subject to the self-quenching, a paradoxical decrease in fluorescence with increasing concentration. The fluorescent molecules may accumulate in the secretory vesicle at a high concentration and thereby show the self-quenching effect. Upon exocytosis, the concentration of fluorescent molecules would decrease dramatically, and thus the quenching effect might vanish, leading to a flash before the fluorescent probes diffuse out. We estimated the concentration of dye in the vesicle to be 10 to 100 μM (see Appendix). This was lower than the concen-

tration at which the self-quenching of the dye becomes significant. Therefore, dequenching of the fluorescent probe by dilution upon the release was unlikely to cause the flash response.

Channels on the vesicles

The K^+ channels present on the vesicle membrane (Fig. 8) may be activated when the intracellular Ca^{2+} concentration rises. This would establish a positive potential inside the vesicle as the vesicular $[K^+]_v$ is less than intracellular $[K^+]_i$. The fusion of a vesicle with the plasma membrane during cell depolarization would result in depolarization of the vesicle membrane also. Thus, the voltage-dependent Cl^- channel (ClC-3), also present on the vesicle membrane (Figs. 6–8), could be activated. Because the intracellular Cl^- concentration, $[Cl^-]_i$, is also higher than that in intravesicular space, $[Cl^-]_v$, KCl salts rapidly accumulate in the vesicular space. This elevates the osmotic tension inside the vesicular space and induces a water transport through the vesicular membrane to the extracellular milieu. Stanley and Ehrenstein (1985) found the K^+ channel in the vesicle membrane by electrical measurement and proposed a similar hypothesis. In their model, the Cl^- channel is open all the time, allowing the vesicle to swell upon the intracellular Ca^{2+}-transient before exocytosis. We hypothesize that the Cl^- channel opens after the exocytotic membrane fusion. Ions and osmosis involved in the water secretion here are comparable with those in various exocrine cells. The osmotic tension further rises as the matrix inside the vesicle is somehow dissolved into the invading water. This generates an ejecting force through a narrow fusion pore, which altogether drives the catecholamine out of the vesicles in a rather straight fashion. Mimicking catecholamine, the fluorescent probe also runs across the exponentially rising evanescent field, which appears as the flash response. The reason why a large increase in membrane conductance has not been recorded during exocytosis (Chow et al., 1996) should be quested further.

The lack of flash or spike in some vesicles might be explained by assuming that these vesicles lost the fluorescent probe upon exocytosis by simple diffusion through the fusion pore without ejection of the water. The fluorescence we measured reflected a balance between the decreasing concentration of dye and the increased intensity of the excitation field. The fluorescent probe released by simple diffusion did not move preferentially toward the glass (in the direction of the objective lens) and thus made no flash response (see Appendix). In fact, the densities of ion channels on the vesicle membrane responsible for water secretion vary from vesicle to vesicle (Fig. 8). This accounts for the variability of the flash response and the S/D ratio.

Cl^- channels have also been found in vesicles of pancreatic β-cell (Barg et al., 1999). The Cl^- channel blockers inhibited exocytosis in human platelets (Pollard et al., 1977), bovine parathyroid cells (Brown et al., 1979), pancreatic islet cells (Pace and Smith, 1983), and isolated bovine adrenal chromaffin cells (Pazoles and Pollard, 1978). DIDS has been reported to have an inhibitory effect on synaptic transmission (Kumamaru et al., 1999). These observations are consistent with our results. The inhibition of the flash responses was probably a result of suppression of the Cl^- flux into the vesicle, which led to suppression of the water flux through the vesicle membrane.

Water flow and its physiological significance

In the process of free diffusion, solute and solvent molecules move in opposite directions without involving a volume flow. The free diffusion has long been thought to be the basis for release of transmitters and hormones from cells into the extracellular milieu. However, the results described above indicate that 1) the exocytotic release of substances is accompanied by a volume flow of water and 2) the release of transmitter occurs in a vectorial fashion, which is susceptible to Cl^- channel blockers. These findings support the idea that the release of transmitters from secretory vesicles is not driven solely by simple diffusion but also by ejection of water. In exocrine cells, it is known that secretion of enzymes and mucus by exocytosis is commonly associated with secretion of water. We demonstrated here that, in endocrine cells also, a similar but localized secretion of water serves to flush the content of secretory vesicles out. This water flow through the vesicle membrane may be necessary to dissolve the densely precipitated signal molecules inside the chromaffin vesicle (0.6 M of catecholamine plus 0.2 M of ATP; Winkler, 1976; Winkler and Westhead, 1980). The water secretion from an endocrine cell leads to a slight decrease in cell volume, which is necessary for the cell to accommodate superfluous patches of the plasma membrane (formed by frequent fusion of exocytotic vesicles) as an invagination. The water secretion and the cell shrinkage favor for a rapid transport of secretes through the intercellular space to the capillary. When a target is nearby, the water flow associated with exocytosis may facilitate the transport of signal molecules to their target sites and then carry them away from the target sites to terminate their action in a short time. The water secreted from the site of exocytosis can be recycled to the same cell through the membrane where no exocytosis has occurred.

Micro secretion of water from endocrine cells and its role would be studied further by DIC microscopy, which allows us to observe shrinkage of the cell, intracellular formation of large vacuoles, and other responses related to the secretion. The force associated with the water flow would be studied more quantitatively by atomic force microscopy in future.

APPENDIX

pH dependence of the fluorescence of acridine orange

The fluorescence intensities of acridine orange solution (3 μM) were measured at two pH levels using a standard cuvette (10 mm) and a fluorescence spectrophotometer (F-4010, Hitachi, Tokyo, Japan). The intensities were 147.6 at pH 7.3 and 150.5 at pH 2.0, and there was very little change in the peak wavelength.

Concentration dependence of the fluorescence of acridine orange

To estimate the concentration of the dye molecules in the vesicle, we compared the fluorescence intensity of vesicles with that of a dye solution placed in the same evanescent field. To compare appropriately, the cells were pressed to the glass substrate with a fine glass rod. This manipulation increased the fluorescence intensity in most vesicles by 60%, indicating that the vesicles docked to the plasma membrane were normally located at ~50 nm or shorter from the glass surface. The maximal fluorescence of the vesicles was recorded for comparison with calibrating solution. Then, the calibrating solution containing a known concentration of acridine orange (10, 50, or 100 μM) was placed in the same dish, and the fluorescence in the region devoid of cells was recorded. By comparing both records, the concentration in most of the vesicles was estimated to be 10 to 30 μM. There were a few extremely bright vesicles, but their concentrations were still lower than 100 μM.

Meanwhile, the fluorescence intensity of the aqueous solution containing acridine orange (1–100 μM) was measured with a fluorescence spectrophotometer (Fig. 9). The fluorescence intensity of dimethyl sulfoxide containing acridine orange at a series of concentrations (1 μM–10 mM) was also measured with our evanescent-wave microscope using an avalanche photodiode (C5460, Hamamatsu Photonics) as a detector. The fluorescence was linearly proportional to the concentration up to ~100 μM in water (Fig. 9, closed circles) and to 10 mM in dimethyl sulfoxide (Fig. 9, open circles).

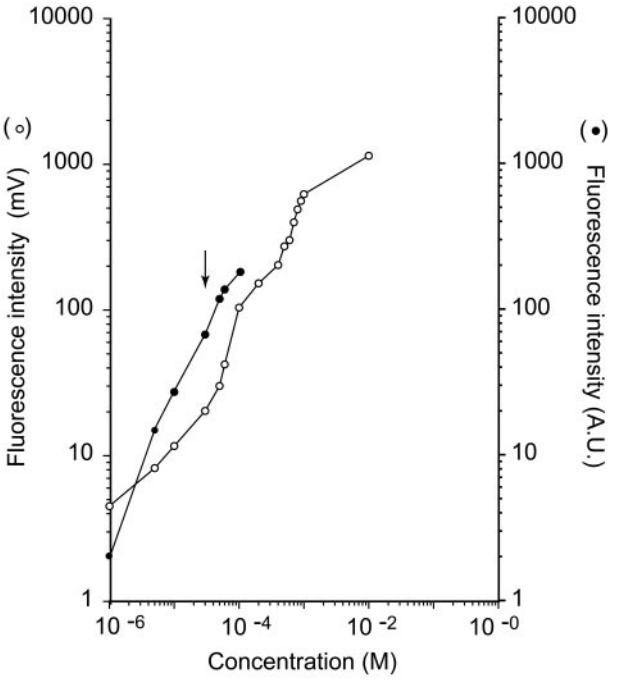

FIGURE 9 Relationship between the intensity of fluorescence and the concentration of acridine orange. Open circles represent data from acridine orange dissolved in dimethyl sulfoxide. The fluorescence intensities were measured with the evanescence microscope using an avalanche photodiode as a detector. The ordinate indicates the value of DC output from the avalanche photodiode. Closed circles represent data from acridine orange dissolved in water. The fluorescence was measured with a fluorescence spectrophotometer (F-4010, Hitachi, Tokyo, Japan) for these data. The arrow indicates the maximal estimated concentration of dye in the vesicle.

Dye molecule distribution simulated by the Monte-Carlo method

We assumed that distribution of dye molecules are determined by Brownian fluctuation of water in a confined space. Release was treated as a drift of 100 dye molecules from a fusion pore on the cell membrane in a random walk in a two-dimensional plane (x-z plane). Individual molecules emit fluorescence with intensity proportional to the field intensity determined by the z coordinate of the molecules. In a unit time equal to one video frame interval, these molecules fluctuate and collide with each other and water molecules to change the course of free straight flight. Instead of tracing all these fluctuations, we determined points of collision by the Monte-Carlo method, and used 33 collision points as light-emitting sources during an integration time of one video frame (= 33 ms). Distributions of these collision points (total of 3300 for 100 dye molecules) under three different conditions are shown in Fig. 10.

We assumed the distance between the glass and the cell membrane to be 50 nm and the diameter of vesicle to be 240 nm. We defined the origin (z = 0) to be on the glass surface. The field intensity (I) follows an exponential function:

$$I = I_0 \times \exp(-z/d) \quad (1)$$

in which d is the decay constant (= 50 nm), and I_0 is the laser intensity, which is set at 2.72 for convenience. The field intensity at the cell membrane becomes 1 in this model. Neglecting the travel across the vesicle, each molecule starts from a point randomly selected on the fusion pore (40 nm in width) and then makes a flight until it collides with another dye molecule or a water molecule. This length of straight flight (free path) is determined, in fact, by the density, viscosity, and temperature, but in the present model it is mathematically determined by the function of random numbers (the mean free path = 65 nm).

When the release of molecules occurs with a simple diffusion of dye molecules from the fusion pore, the distribution of molecules outside the cell becomes like the one shown in the middle panel of the Fig. 10. Molecules released from the fusion pore had a mean free path longer than the gap space outside the cell. Therefore, they easily hit the glass surface to bounce back and immediately make a fairy even distribution along the z axis.

When the release occurs with a volume flow of water in addition to the Brownian movement, the dye molecules are drifted toward the glass surface. The maximum velocity of water ejection at the fusion pore is assumed to be 50 nm/ms and to be decreased linearly with the distance from the fusion pore to zero at the glass surface (average velocity = 12 nm/ms). The result of this simulation is shown in the right panel of Fig. 10.

We calculated the total fluorescence intensity of the molecules found in a box defined by two lines l and l' (40-nm wide). If the x value of a molecule at one of its collisions fell in the box (of interest), then the fluorescence intensity of the molecule determined by its z value and Eq. (1) was registered and added to the total intensity of light coming from the box. The fluorescence intensities thus calculated for the center of a vesicle image were 592 (in arbitrary unit) for dye molecules in the vesicle (A), 546 for molecules released only by the Brownian movement (B), and 981 for those released by the Brownian movement plus an extra force of water

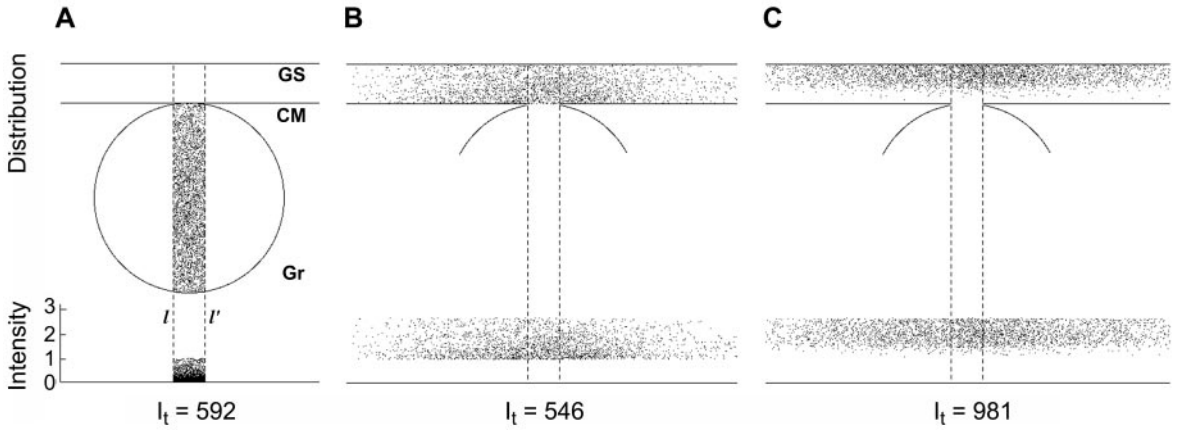

FIGURE 10 Monte-Carlo simulation of the release of fluorescent probes from a secretory vesicle. (*Top*) Distribution of dye molecules in a vesicle before release (*A*), after release by Brownian fluctuation (*B*), and after release by Brownian fluctuation plus water ejection (*C*). One-hundred fluorescent molecules were taken into consideration. These molecules fluctuated as they collided with each other and water molecules 100 times in a unit time of 33 ms, leaving 3300 points of fluorescent sources that could be collected and integrated by the camera to make a frame of image. (*Bottom*) Intensity plot of individual dye molecules depending on their position shown on the top. The integrated intensity (I_t) of fluorescence from molecules located between two lines l and l' is noted under each figure. In *C*, the volume flow of water (in a velocity of $\sim$1.5 μm/s) shifted the position of dye molecules toward the glass in an inverse proportion with the original distance from the cell membrane. A distance of 50 nm between the cover glass and the cell membrane and a diameter of vesicle of 240 nm were assumed. GS, Surface of cover glass; CM, cell membrane; Gr, secretory granule.

ejection (C). Varying the mean free path and other parameters changes these values greatly in a predictable manner.

We thank the staff of a local slaughterhouse for supplying bovine adrenals, and Olympus Optical Co. for the use of LSR's CCD camera. We also thank M. Ohbayashi for help in immunostaining and Dr. Charles Edwards for reading and correcting English text. This study was supported by Grant-in-Aids (10557003 and 11794015 to S. T.; 8701 to T.T.) from the Ministry of Education, Science and Culture, Japan. T.T. was a Research Fellow of the Japan Society for the Promotion of Science (JSPS).

REFERENCES

Ashley, R. H., D. M. Brown, D. K. Apps, and J. H. Phillips. 1994. Evidence for a K^+ channel in bovine chromaffin granule membranes: single-channel properties and possible bioenergetic significance. *Eur. Biophys. J.* 23:263–275.

Barg, S., E. Renstrom, P. O. Berggren, A. Bertorello, K. Bokvist, M. Braun, L. Eliasson, W. E. Holmes, M. Kohler, P. Rorsman, and F. Thevenod. 1999. The stimulatory action of tolbutamide on Ca^{2+}-dependent exocytosis in pancreatic beta cells is mediated by a 65-kDa mdr-like P-glycoprotein. *Proc. Natl. Acad. Sci. U. S. A.* 96:5539–5544.

Best, L., P. D. Brown, E. A. Sheader, and A. P. Yates. 2000. Selective inhibition of glucose-stimulated beta-cell activity by an anion channel inhibitor. *J. Membr. Biol.* 177:169–175.

Bowman, E. J., A. Siebers, and K. Altendorf. 1988. Bafilomycins: a class of inhibitors of membrane ATPases from microorganisms, animal cells, and plant cells. *Proc. Natl. Acad. Sci. U. S. A.* 85:7972–7976.

Brandt, B. L., S. Hagiwara, Y. Kidokoro, and S. Miyazaki. 1976. Action potentials in the rat chromaffin cell and effects of acetylcholine. *J. Physiol. (Lond).* 263:417–439.

Breckenridge, L. J., and W. Almers. 1987. Final steps in exocytosis observed in a cell with giant secretory granules. *Proc. Natl. Acad. Sci. U. S. A.* 84:1945–1949.

Brown, W. M., C. J. Pazoles, C. E. Creutz, G. D. Aurbach, and H. B. Pollard. 1979. Role of anions in parathyroid hormone release from dispersed bovine parathyroid cells. *Proc. Natl. Acad. Sci. U. S. A.* 75:876–880.

Chow, R. H., J. Klingauf, C. Heinemann, R. S. Zucker, and E. Neher. 1996. Mechanisms determining the time course of secretion in neuroendocrine cells. *Neuron.* 16:369–376.

Finkelstein, A., J. Zimmerberg, and F. S. Cohen. 1986. Osmotic swelling of vesicles: its role in the fusion of vesicles with planar phospholipid bilayer membranes and its possible role in exocytosis. *Annu. Rev. Physiol.* 48:163–174.

Gelles, J., B. J. Schnapp, and M. P. Sheetz. 1988. Tracking kinesin-driven movements with nanometre-scale precision. *Nature.* 331:450–453.

Grant, N. J., D. Aunis, and M. F. Bader. 1987. Morphology and secretory activity of digitonin- and alpha-toxin-permeabilized chromaffin cells. *Neuroscience.* 23:1143–1155.

Kawasaki, M., S. Uchida, T. Monkawa, A. Miyawaki, K. Mikoshiba, F. Marumo, and S. Sasaki. 1994. Cloning and expression of a protein kinase C-regulated chloride channel abundantly expressed in rat brain neuronal cells. *Neuron.* 12:597–604.

Kumamaru, E., M. Sato, H. Yoshida, T. Ide, and M. Kasai. 1999. pH-dependent fusion of synaptosomal membrane studied by fluorescence quenching method. *Jpn. J. Physiol.* 49:19–25.

Llopis, J., J. M. McCaffery, A. Miyawaki, M. G. Farquhar, and R. Y. Tsien. 1998. Measurement of cytosolic, mitochondrial, and Golgi pH in single living cells with green fluorescent proteins. *Proc. Natl. Acad. Sci. U. S. A.* 95:6803–6808.

Miyamoto, S., and S. Fujime. 1988. Regulation by Ca^{2+} of membrane elasticity of bovine chromaffin granules. *FEBS Lett.* 238:67–70.

Ohara-Imaizumi, M., Y. Nakamichi, T. Tanaka, H. Ishida, and S. Nagamatsu. 2002. Imaging exocytosis of single insulin secretory granules with evanescent wave microscopy: distinct behavior of granule motion in biphasic insulin release. *J. Biol. Chem.* 277:3805–3808.

Oheim, M., D. Loerke, W. Stuhmer, and R. H. Chow. 1998. The last few milliseconds in the life of a secretory granule: docking, dynamics and fusion visualized by total internal reflection fluorescence microscopy (TIRFM). *Eur. Biophys. J.* 27:83–98.

Ornberg, R. L., S. Furuya, G. Goping, and G. A. Kuijpers. 1995. Granule swelling in stimulated bovine adrenal chromaffin cells: regulation by internal granule pH. *Cell Tissue Res.* 279:85–92.

Pace, C. S., and J. S. Smith. 1983. The role of chemiosmotic lysis in the exocytotic release of insulin. *Endocrinology.* 113:964–969.

Pazoles, C. J., and H. B. Pollard. 1978. Evidence for stimulation of anion transport in ATP-evoked transmitter release from isolated secretory vesicles. *J. Biol. Chem.* 253:3962–3969.

Pollard, H. B., C. J. Pazoles, C. E. Creutz, J. H. Scott, O. Zinder, and A. Hotchkiss. 1984. An osmotic mechanism for exocytosis from dissociated chromaffin cells. *J. Biol. Chem.* 259:1114–1121.

Pollard, H. B., C. J. Pazoles, C. E. Creutz, and O. Zinder. 1980. Role of intracellular proteins in the regulation of calcium action and transmitter release during exocytosis. *Monogr. Neural. Sci.* 7:106–116.

Pollard, H. B., K. Tack-Goldman, C. J. Pazoles, C. E. Creuts, and N. R. Shulman. 1977. Evidence for control of serotonin secretion from human platelets by hydroxyl ion transport and osmotic lysis. *Proc. Natl. Acad. Sci. U. S. A.* 74:5295–5299.

Schmoranzer, J., M. Goulian, D. Axelrod, and S. M. Simon. 2000. Imaging constitutive exocytosis with total internal reflection fluorescence microscopy. *J. Cell Biol.* 149:23–32.

Stanley, E. F., and G. Ehrenstein. 1985. A model for exocytosis based on the opening of calcium-activated potassium channels in vesicles. *Life Sci.* 37:1985–1995.

Steyer, J. A., H. Horstmann, and W. Almers. 1997. Transport, docking and exocytosis of single secretory granules in live chromaffin cells. *Nature.* 388:474–478.

Stout, A. L., and D. Axelrod. 1989. Evanescent field excitation of fluorescence by epi-illumination microscopy. *Appl. Optics.* 28:5237–5242.

Terakawa, S., J. H. Fan, K. Kumakura, and M. Ohara-Imaizumi. 1991. Quantitative analysis of exocytosis directly visualized in living chromaffin cells. *Neurosci. Lett.* 123:82–86.

Terakawa, S., S. Manivannan, and K. Kumakura. 1993. Evidence against the swelling hypothesis for initiation of exocytosis in terminals of chromaffin cell processes. *J. Physiol. (Paris).* 87:209–213.

Terakawa, S., T. Sakurai, and K. Abe. 1997. Development of an objective lens with a high numerical aperture for light microscopy. *Bioimages.* 5:24.

Thirion, S., J. D. Troadec, N. B. Pivovarova, S. Pagnotta, S. B. Andrews, R. D. Leapman, and G. Nicaise. 1999. Stimulus-secretion coupling in neurohypophysial nerve endings: a role for intravesicular sodium? *Proc. Natl. Acad. Sci. U. S. A.* 96:3206–3210.

Tokunaga, M., K. Kitamura, K. Saito, A. H. Iwane, and T. Yanagida. 1997. Single molecule imaging of fluorophores and enzymatic reactions achieved by objective-type total internal reflection fluorescence microscopy. *Biochem. Biophys. Res. Commun.* 235:47–53.

Toomre, D., J. A. Steyer, P. Keller, W. Almers, and K. Simons. 2000. Fusion of constitutive membrane traffic with the cell surface observed by evanescent wave microscopy. *J. Cell Biol.* 149:33–40.

Walsh, K. B., K. J. Long, and X. Shen. 1999. Structural and ionic determinants of 5-nitro-2-(3-phenylprophyl-amino)-benzoic acid block of the CFTR chloride channel. *Br. J. Pharmacol.* 127:369–376.

Warashina, A. 1985. Changes in the size of isolated chromaffin granules in ATP-evoked catecholamine release. *FEBS Lett.* 184:87–89.

Waymire, J. C., W. F. Bennett, R. Boehme, L. Hankins, K. Gilmer-Waymire, and J. W. Haycock. 1983. Bovine adrenal chromaffin cells: high-yield purification and viability in suspension culture. *J. Neurosci. Methods.* 7:329–351.

Winkler, H. 1976. The composition of adrenal chromaffin granules: an assessment of controversial results. *Neuroscience.* 1:65–80.

Winkler, H., and E. Westhead. 1980. The molecular organization of adrenal chromaffin granules. *Neuroscience.* 5:1803–1823.

Xu, T., T. Binz, H. Niemann, and E. Neher. 1998. Multiple kinetic components of exocytosis distinguished by neurotoxin sensitivity. *Nat. Neurosci.* 1:192–200.

Zimmerberg, J., M. Curran, F. S. Cohen, and M. Brodwick. 1987. Simultaneous electrical and optical measurements show that membrane fusion precedes secretory granule swelling during exocytosis of beige mouse mast cells. *Proc. Natl. Acad. Sci. U. S. A.* 84:1585–1589.